Kinetics of Austenite-Ferrite and Austenite-Pearlite Transformations in a 1025 Carbon Steel

E. B. HAWBOLT, B. CHAU, and J. K. BRIMACOMBE

Isothermal and continuous-cooling transformation kinetics have been measured dilatometrically for the $\gamma \rightarrow \alpha + \gamma'$ and $\gamma' \rightarrow P$ reactions in a 1025 steel. The isothermal transformation of austenite for each reaction was found to fit the Avrami equation after the fraction transformed was normalized to unity at the completion of the reaction and a transformation-start time was determined. The transformation kinetics under isothermal conditions therefore were characterized in terms of the n and b parameters from the Avrami equation together with the transformation-start times. The parameter n was found to be independent of temperature over the range studied (645 to 760 °C) and to have values of 0.99 and 1.33 for the ferrite and pearlite reactions, respectively. This indicates that the nucleation condition is essentially constant and site saturation occurs early in the transformation process. The continuous-cooling experiments were conducted at cooling rates of 2 to 150 °C per second to determine the transformation-start times for the ferrite and pearlite reactions and the completion time for transformation to pearlite under CCT conditions. Both reactions were found to obey the Additivity Principle for continuous cooling provided that the incubation (pre-transformation) period was not included in the transformation time. The isothermal transformation data and CCT transformation-start times have been incorporated in a mathematical model to predict continuous-cooling transformation kinetics that agree closely with measurements made at three cooling rates.

I. INTRODUCTION

THE steel industry is rapidly adopting continuous processes including continuous casting, continuous annealing, and continuous heat treatment to minimize production costs and to improve control of product quality. The achievement of optimum processing conditions for producing steel with the desired properties can be assisted by the development of mathematical models that link the composition and thermomechanical treatment of the steel to its final mechanical properties. Thus, a program has been established at The University of British Columbia to develop a model of industrial heat-treatment processes such as Stelmor.

The mathematical model requires accurate data on the phase-transformation kinetics of different steels. In a previous paper[1] the isothermal and continuous-cooling decomposition kinetics of austenite to pearlite in a eutectoid, plain-carbon steel were reported. These data then were employed to show the validity of applying the Additivity Principle to predict continuous-cooling transformation kinetics from isothermal-transformation measurements, as described by the Avrami equation[2]*

* Symbols are described at the end of the paper.

$$X = 1 - \exp(-bt^n) \qquad [1]$$

and a measured initiation time for the continuous-cooling conditions. Thus, at least for the eutectoid steel, isothermal data in combination with the Additivity Principle can be employed with confidence in the mathematical model.

The model also consists of heat-flow equations, as described by Agarwal and Brimacombe,[3] so that the transient distributions of temperature and fraction transformed can be predicted simultaneously in shapes such as rods routinely cooled on a Stelmor line. The validity of the model has been confirmed by Iyer[4] by comparing model predictions to measurements of transient temperature at the centerline of 9 to 10 mm diameter rods subjected to forced-air cooling.

Tamura *et al.*[5,6] also have developed models to predict transformations in steel, in which the Avrami equation is employed to characterize the isothermal decomposition of austenite to pearlite or bainite and the Additivity Principle is applied. In their characterization of the isothermal decomposition kinetics, the incubation (pre-transformation) period is combined with the transformation time to obtain the necessary kinetic parameters, n and b (Eq. [1]), from data in the literature. However, our study has shown that only the transformation event fulfills the criteria of the Additivity Principle, *viz.*, dependence solely on the fraction transformed and transformation temperature. Thus inclusion of the incubation period in the calculation of continuous-cooling transformation kinetics from isothermal data inevitably will lead to errors. Isothermal kinetic parameters should be calculated based on an initial time corresponding to the start of transformation rather than the instant that the temperature drops below T_{A_1} as proposed by Tamura *et al.*

The Additivity Principle was suggested originally by Scheil[7] for the prediction of the incubation period of a continuous-cooling transformation. Mathematically it can be stated as follows:

$$\int \frac{dt}{\tau} = 1 \qquad [2]$$

However, in the previous study,[1] the authors have found that the initiation time for transformation is seriously overestimated by Eq. [2] as compared to the experimentally measured transformation start time for the eutectoid, plain-carbon steel. Thus it was necessary to include in the transformation model a relationship describing the effect of continuous-cooling rate on the transformation start time.

E. B. HAWBOLT, Professor, B. CHAU, Research Engineer, and J. K. BRIMACOMBE, Stelco Professor of Process Metallurgy, are with The Centre for Metallurgical Process Engineering, Department of Metallurgical Engineering, The University of British Columbia, Vancouver, BC V6T 1W5, Canada.

Manuscript submitted July 11, 1984.

Kirkaldy *et al.*[8,9] have combined thermodynamic and kinetic parameters to obtain mathematical relationships describing the continuous-cooling transformation event. But the incubation time for continuous cooling was calculated by a procedure which results in a value in excess of that predicted by the Scheil equation.

A curve-fitting technique has been adopted by Blondeau *et al.*[10] at Creusot-Loire in which a large number of CCT diagrams have been reduced to mathematical equations. By combining the thermal history to a given CCT diagram the weight fraction of each component phase — ferrite, pearlite, bainite, martensite — can be predicted and the average hardness and mechanical properties derived. However, the resulting empirical equations have not been coupled with heat flow equations so that specification, rather than calculation, of the transient temperature distribution is necessary.

Research is continuing at U.B.C. to combine the heat flow and transformation kinetics with transformation temperature, pearlite spacing, and mechanical property relationships[11,12] in a fully predictive mathematical model. Once completed, it will be possible to predict the appropriate Stelmor cooling conditions, for example, to optimize the resulting mechanical properties of steel rod undergoing controlled cooling.

As part of this program to develop appropriate transformation models, the use of the Avrami equation to characterize both the austenite-ferrite and austenite-pearlite transformation in hypoeutectoid, plain-carbon steels has been examined for a 1025 steel.* Here the Avrami equation has been used to describe empirically the sigmoidal shape of the transformation curves. In this study, accurate kinetic measurements of the isothermal and the continuous-cooling decomposition of austenite to ferrite and pearlite have been made; accurate data are necessary to test the model as combined isothermal and continuous-cooling kinetics for a steel of given composition and austenitizing condition are not readily available in the literature. In addition, the previous study on eutectoid steels[1] established the necessity for using thin steel specimens and rapid temperature change procedures to ensure that the measurement of isothermal kinetics was not affected by the transformation initiating prior to the attainment of the isothermal transformation temperature and that transformation gradients were minimized within the test specimen.*

* Similar experiments using a 1040 and a 1060 steel are currently being completed.

* Commercial dilatometer devices often use 3 mm diameter specimens whereas our sample has a wall thickness of 0.8 mm thereby significantly reducing temperature gradients during transformation.

The isothermal kinetics for the $\gamma \rightarrow \alpha + \gamma'$ and $\gamma' \rightarrow P$ have been described in terms of the Avrami parameters n_F and b_F and n_P, b_P, respectively. In addition, the experimental fraction of ferrite formed $X_{F_E}(T)$, as a function of the transformation temperature, has also been measured. The application of the additivity condition to the continuous decomposition of austenite to ferrite and pearlite then has been examined. A relationship for the CCT start time, $t_{\mathrm{Av}_{\mathrm{CCT}}}$, as a function of continuous-cooling rate also has been developed. Next, the experimental parameters, n_F, b_F, n_P, b_P, $X_{F_E}(T)$, and $t_{\mathrm{Av}_{\mathrm{CCT}}}$ have been employed in a mathematical model to predict the transformation kinetics for a range of continuous-cooling conditions extending to 23 °C per second. The results have been compared with the measured kinetics obtained from an expansion analysis of the continuous-cooling dilatometric data to validate the model.

II. EXPERIMENTAL

A. *Apparatus and Material*

The isothermal and continuous-cooling transformation measurements were made using the dilatometer shown in Figure 1. The dilatometer is the same as that employed for measurements on the eutectoid steel,[1] although a slight modification was made to the cooling system to elevate achievable cooling rates to 300 °C per second. Diametral dimensional changes are monitored by a water-cooled, quartz-tipped extensometer, while the temperature at the same axial location is measured with an intrinsic, chromel-alumel thermocouple spot-welded to the surface of the steel specimen. Tubular 1025 steel specimens, with dimensions of 8 mm OD by 100 mm length and having a wall thickness of 0.8 mm, were employed in the experiments to minimize radial temperature gradients. A special procedure, which has been described previously,[1] was developed for fabrication of the specimens to ensure that the wall thickness was uniform. For transformation measurements, the steel was resistively heated. Cooling at rates up to 160 °C per second was achieved by flowing helium over the internal and external surfaces of the specimens. Higher cooling rates, approaching 300 °C per second, were obtained by incorporating a water aspirator which injects a fixed amount of water spray through the tubular specimens. Low cooling rates down to 2 °C per second, required for some CCT tests, were attained by a combination of reduced helium flow and low current input to the steel specimen. During the tests the steel specimens were maintained in an inert helium atmosphere.

The composition of the 1025 steel rod from which the test specimens were machined is given in Table I. The austenite grain size is also included.

B. *Equipment Evaluation*

1. *Temperature measurements*

The accuracy of the thermocouple measurements was checked by heating a specimen of the 1025 steel at a rate of ~2 °C per second, to the vicinity of the A_{c_1} temperature, then continuing heating to the A_{c_3} temperature. The temperature and diameter of the specimen were monitored simultaneously. Thus it was found that the A_{c_1} temperature was 723 ± 2 °C and the A_{c_3} temperature was 815 ± 2 °C. These values are in agreement with the equilibrium transformation temperatures of 724.2 and 816.7 °C, respectively, calculated from published correlations based on the steel composition.[13]

2. *Dimension measurement*

The accuracy of the dilatometer measurement was evaluated by measuring the expansion coefficient of ferrite in Armco iron, and of pearlite and austenite in a eutectoid steel. As reported previously,[1] the results agreed closely with values in the literature.

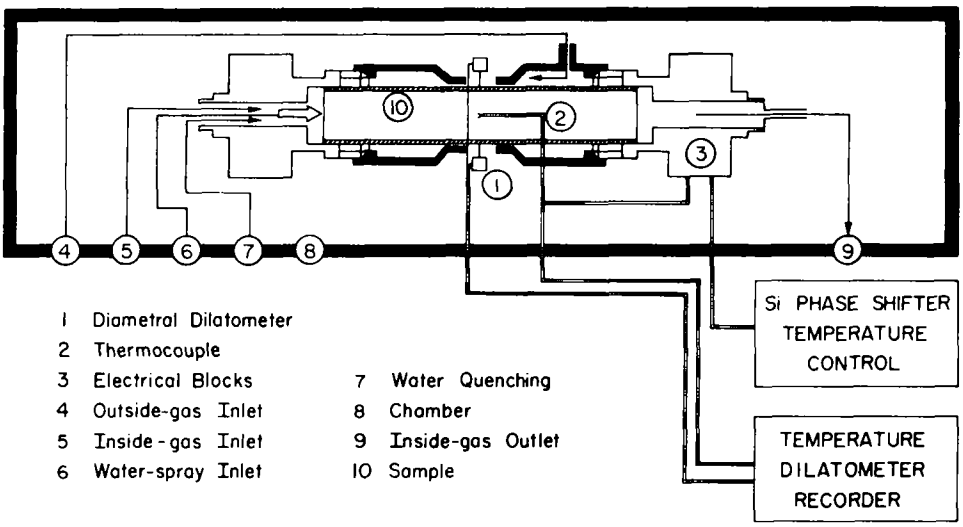

Fig. 1 — Schematic diagram of dilatometer employed for measurement of transformation kinetics.

Table I. Composition of 1025 Steel Used in Transformation Tests (Wt Pct) (γ Grain Size ASTM: 8-9)

C	Mn	Si	S	P
0.25	0.46	0.21	0.014	0.018

C. *Procedure*

1. *Isothermal tests*

For the isothermal tests, the specimens were austenitized by resistance heating in a helium atmosphere to 880 °C and holding for 180 seconds. Normally the specimens then were cooled with helium at a rate of 150 °C per second to the desired temperature, whereupon resistive heating was applied to achieve isothermal conditions. However, at the lower test temperature, approaching 640 °C, the specimens were cooled at about 300 °C per second with both helium and the internal water spray to avoid transformation during the cooling period. Owing to the rapid transformation rate and concomitant evolution of latent heat at the lower test temperature, the helium flow rate had to be raised during the isothermal period to minimize recalescence. In high-temperature tests above T_{A_1} the specimens also were helium-cooled at 150 °C per second to the test temperature; and after the $\gamma \rightarrow \alpha + \gamma'$ transformation was completed, as determined from the sigmoidal curve generated by the dilatometer, the specimens were rapidly cooled to room temperature using the water quench.

2. *Continuous cooling*

In the continuous-cooling tests, the specimens were cooled from 880 °C using helium, sometimes with the application of reduced resistive heating to attain the desired cooling rate which ranged from 2 to 150 °C per second (as measured at T_{A_1}). In all transformation tests the outputs from the specimen thermocouple and dilatometer were recorded simultaneously.

3. *Metallographic studies*

Quantitative metallography using a Wild Leitz Image Analyzer System was also employed to determine the extent of the $\gamma \rightarrow \alpha$ transformation for the lower temperature isothermal tests and for the continuous-cooling experiments.

III. RESULTS AND DISCUSSION

A. *Isothermal Measurements*

1. *Transformations above T_{A_1}*

The isothermal transformation of austenite to proeutectoid ferrite at temperatures above T_{A_1} exhibits a typical sigmoidal dependence on time as shown in Figure 2(a). Therefore the transformation kinetics could be described by the Avrami equation. The parameters n and b in the Avrami

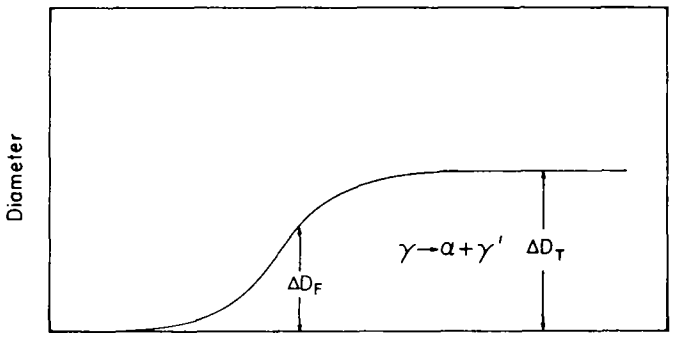

(*a*)

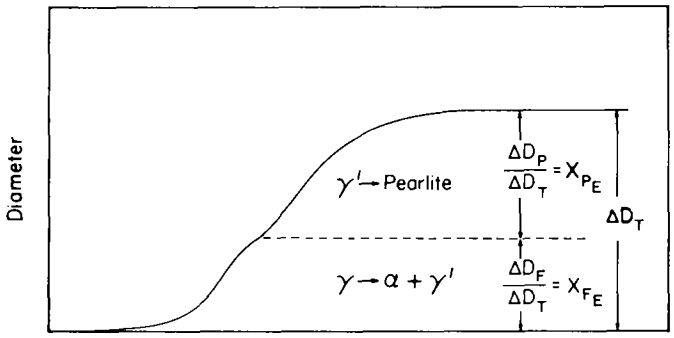

(*b*)

Fig. 2 — Schematic isothermal, diametral dilatometer curves showing the decomposition of austenite: (*a*) to proeutectoid ferrite, as occurs above T_{A_1}; (*b*) to ferrite then pearlite, as occurs below T_{A_1}.

Table II. Calculated Weight Fraction of Ferrite, W_F, Corrected to Volume Fraction, X_{F_C}, and Compared with the Metallographic, X_F° and Dilatometric, X_{F_E} Observations

Temperature	W_F (Calculated Weight Fraction of Ferrite)	$X_{F_C}^*$ (Volume Fraction Calculated from W_F)	X_F° (Volume Fraction Ferrite Obtained by Metallography)	X_{F_E} $\left(\frac{\Delta D_F}{\Delta D_T}\right)$
760	0.555	0.553	0.545	0.548
750	0.600	0.598	0.603	0.600
740	0.646	0.645	0.641	0.642
T_{A_1}(724)	0.695	0.694	—	—
720	0.690	0.689	0.686	0.687
709	0.679	0.678	0.668	0.670
690	0.657	0.656	0.653	0.652
680	0.645	0.644	0.633	0.635
670	0.632	0.631	0.612	0.615
661	0.620	0.619	0.592	0.595
645	0.597	0.595	0.560	0.565

*W_F has been corrected to X_{F_C} using $\rho_F = 7.86$ and $\rho_P = 7.81$ g/cm^3.

equation were obtained from a least-squares fit of the kinetic data to a plot of ln ln$[1/(1 - X)]$ *vs* ln t. However, because the total fraction of ferrite formed at a given temperature was less than 1 whereas the Avrami equation is based on a total fraction of unity, the transformation data had to be normalized before the least-squares fit was made. Thus the measured volume fraction transformed at each time was divided by the total volume fraction transformed, measured at the end of the transformation, X_{F_E}. Since the volume fraction transformed is linearly proportional to the change in diameter of the test specimen, ΔD_F, the normalizing was accomplished by dividing ΔD_F by ΔD_T, the overall diameter change after completion of transformation.

The total amount of ferrite formed at each isothermal test temperature also was determined by quantitative metallographic examination of the specimen following the test. This value was in good agreement with the volume fraction of ferrite calculated from the total measured ΔD_T, as shown in Table II.

To determine the start of transformation, $t = 0$ was selected initially as the time at which the sample cooled below the A_3 temperature. The initiation time then was increased by small increments (0.1 second) until the best fit for the ln ln$[1/(1 - X)]$ *vs* ln t line was obtained by a least-squares analysis. The transformation start time giving the best fit was designated as "t-Avrami ferrite" or t_{AV_F}.

2. *Transformations below T_{A_1}*

At temperatures below T_{A_1}, the austenite partially decomposes to ferrite accompanied by an increase in the carbon content of the remaining austenite. The transformation continues with the higher carbon austenite transforming to pearlite. A typical dilatometric decomposition curve is shown in Figure 2(b).

At the lower test temperatures, 661 °C and 645 °C, some recalescence was observed. The "isothermal" temperature, therefore, was taken to be the average of the temperature observed during the transformation. In these tests the dilatometric data were corrected for thermal expansion. This was accomplished by estimating the fraction transformed from the experimental dilatometric curve, then calculating the thermal expansion associated with each of the phases present and subtracting it from the dilatometric curve. The procedure was repeated iteratively.

The isothermal tests confirmed that the total volume fraction of ferrite decreases with decreasing transformation temperature below T_{A_1}, as shown by the dilatometric volume fraction of ferrite, $X_{F_E} = \Delta D_F/\Delta D_T$ and the metallographic observations reported in Table II. To rationalize the transformations that are occurring at temperatures below the boundaries of the equilibrium phase diagram, as a first approximation, the γ/Fe_3C and α/γ equilibrium phase boundaries of the Fe-C phase diagram were linearly extrapolated to lower temperatures as shown in Figure 3. Previously, equilibrium phase boundaries have been extrapolated by Kaufman *et al.*[14] to examine the thermodynamics of the bainite transformation.

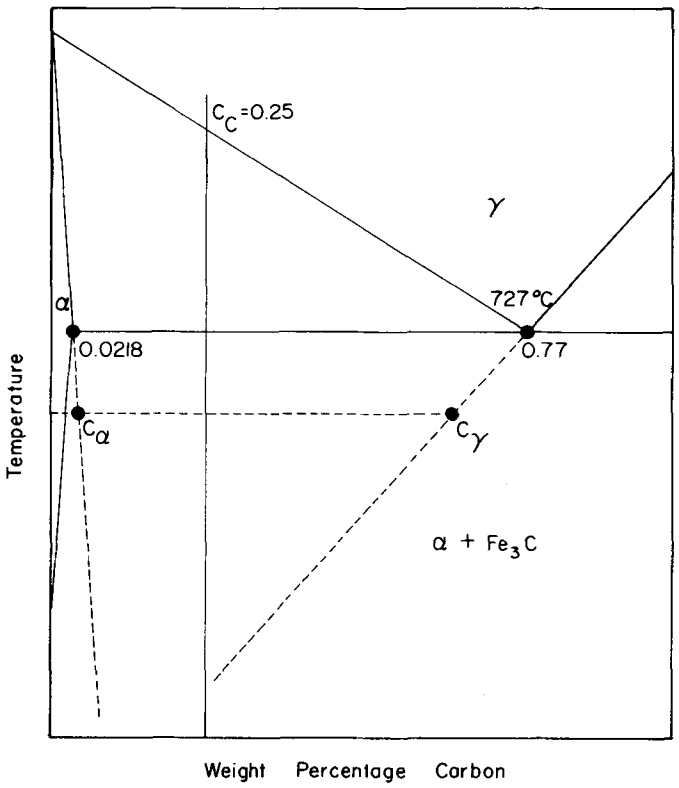

Fig. 3—Schematic Fe-C phase diagram showing the extrapolated γ/Fe_3C and α/γ phase boundaries.

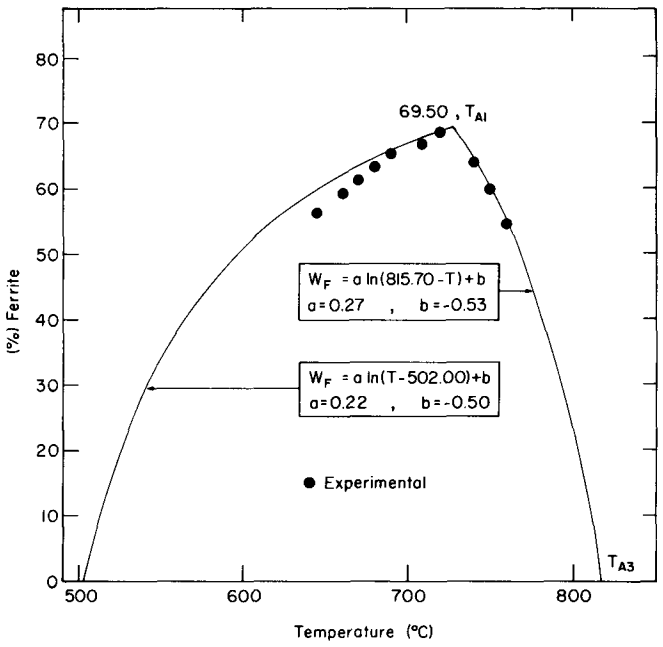

Fig. 4 — Percent ferrite at each transformation temperature calculated using the extrapolated Fe-C phase boundaries and compared with the quantitative metallographic and dilatometer observations.

The resulting phase boundaries were used with the lever law to calculate the weight fraction of ferrite at each temperature, as shown in Figure 3, *e.g.*, at T_1.

$$W_F = \frac{C_\gamma - C_C}{C_\gamma - C_\alpha} \text{(wt fraction)} \qquad [3]$$

The weight fraction has been converted to volume fraction, X_{F_C}, using the densities of the ferrite and pearlite phases; and the results are included in Table II. The data are also shown in Figure 4 together with the equations describing the calculated W_F for temperatures extending from T_{A_3} down to 500 °C. Reasonable agreement is seen between the experimental (metallographic plus dilatometric) results and the calculated values, although the latter are consistently higher and the deviation increases with decreasing temperature.

3. *Kinetics of ferrite and pearlite transformations*

Although two distinct transformation events are visible in Figure 2(b), the transition between the ferrite and pearlite transformation does not reflect the sigmoidal shape characteristic of the individual reactions. This is consistent with the $\gamma \rightarrow \alpha + \gamma'$ reaction continuing for a short time after the onset of the pearlite reaction. To reflect this loss of sigmoidal behavior in the ferrite/pearlite transition region, the fraction of ferrite must be normalized by a value which is slightly larger than the observed experimental $\Delta D_F/\Delta D_T$ (Figure 2). Therefore the calculated volume fraction of ferrite based on the extrapolated phase boundaries has been used to normalize the experimental X_F to 1.0,* as follows:

*Experiments involving 0.4 and 0.6 carbon steels are currently underway and the resulting data are being used to locate better the phase boundaries below T_{A_1}. An alternative approach in which the $\gamma \rightarrow \alpha$ transformation is assumed to continue for an additional 0.01 wt fraction after the start of the pearlite transformation also could be followed.

$$X_F = \frac{\Delta D_F/\Delta D_T}{X_{F_C}} \qquad [4]$$

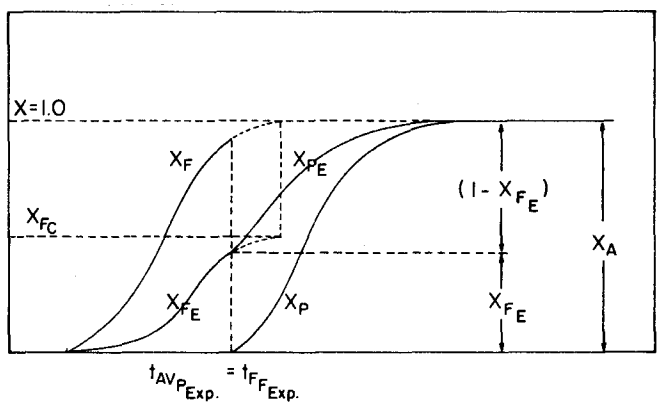

Fig. 5 — Schematic dilatometer response showing the basis of normalization of the volume fraction of each constituent phase to 1.0 which was necessary to calculate the corresponding n and b kinetic parameters for each transformation.

The experimental volume fraction of pearlite transformed for a given temperature was normalized to unity as follows:

$$X_P = \frac{\Delta D_P/\Delta D_T}{1 - X_{F_E}} \qquad [5]$$

since all of the remaining austenite transforms to pearlite. The details of the normalization are shown in Figures 2 and 5.

The "start time" for the ferrite transformation, t_{AV_F}, was determined from the kinetics data by the same procedure followed for the proeutectoid ferrite described earlier. The same method was adopted for the pearlite transformation, with the experimental transition time between the two transformations being taken as the initial $t = 0$ for the reaction. The resulting transformation start times are in good agreement (within 1 second) with the values observed on the dilatometric transformation curves.

The n and b parameters for each transformation were calculated on the basis of the individual transformation start times, t_{AV_F} and t_{AV_P}, where:

$$X_F = 1 - \exp[-b_F(t - t_{AV_F})^{n_F}] \qquad [6]$$

and

$$X_P = 1 - \exp[-b_P(t - t_{AV_P})^{n_P}] \qquad [7]$$

where t_{AV_P} is the experimentally observed time of completion of the ferrite transformation. The resulting isothermal n and b parameters are characteristic of the transformation kinetics only and not the combined incubation plus transformation event. Figure 6 shows that for both the ferrite and pearlite transformations n is effectively independent of the isothermal-transformation temperature. This indicates that the nucleation site is unchanging over the measured transformation range of 645° to 760 °C. This is an important requirement to be met if the instantaneous transformation rate is to be a function only of the fraction transformed and the transformation temperature; a constant n has been shown to be consistent with the additivity requirements.[1]* The iso-

*Tamura *et al.*[5,6] base their calculation for the eutectoid austenite-to-pearlite transformation on $t = 0$ at T_{A_1}. The resulting kinetic parameter, n, is then a function of temperature, whereas Agarwal and Brimacombe[3] have shown that the Additivity Principle holds if n is a constant, independent of temperature.

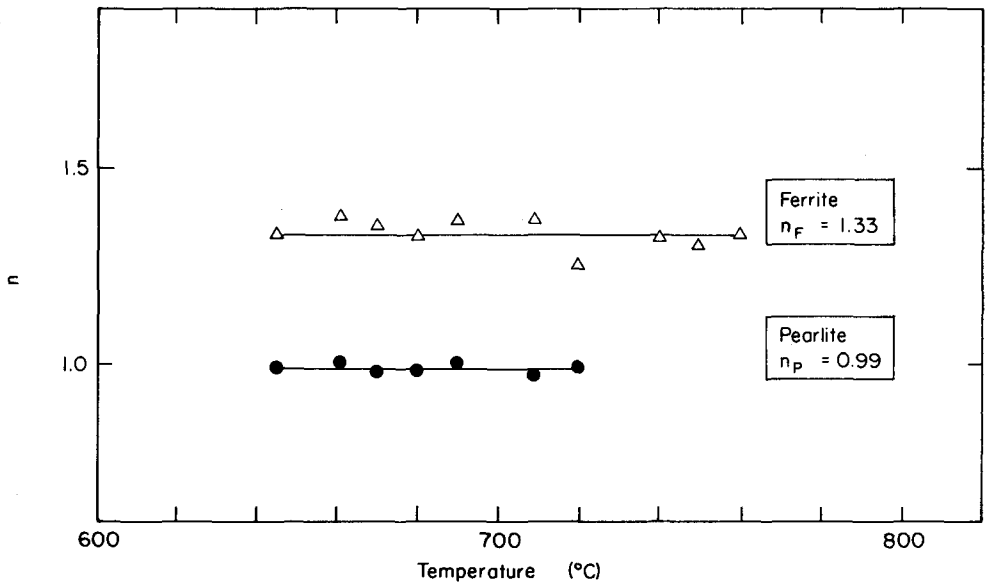

Fig. 6—Calculated kinetics parameter, n, plotted against transformation temperature for the $\gamma \rightarrow \alpha + \gamma'$ and the $\gamma' \rightarrow$ pearlite transformations.

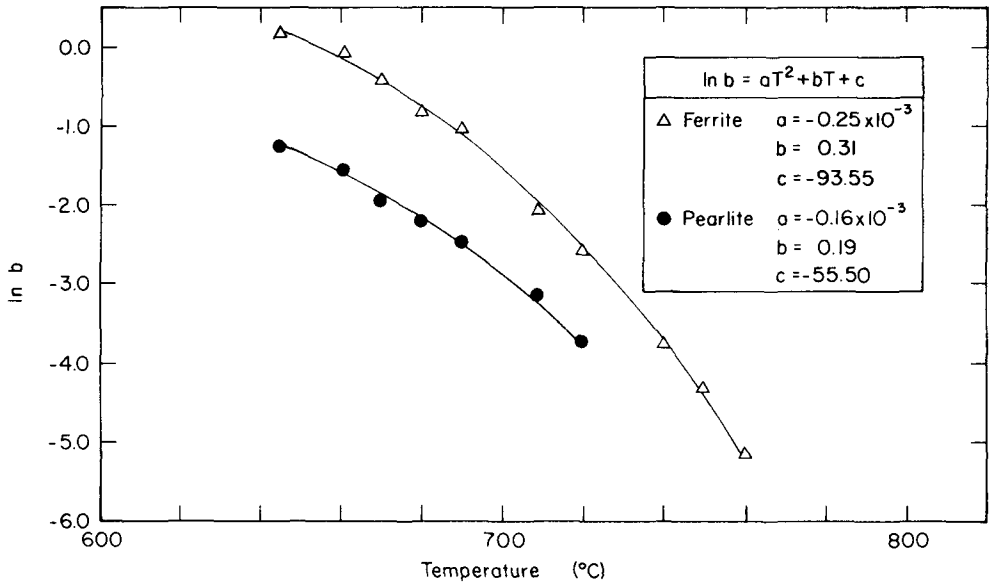

Fig. 7—Calculated kinetics parameter, b, plotted against transformation temperature for the $\gamma \rightarrow \alpha + \gamma'$ and the $\gamma' \rightarrow$ pearlite transformations.

thermal data of b *vs* the transformation temperature for the $\gamma \rightarrow \alpha + \gamma'$ and the $\gamma' \rightarrow$ pearlite transformation are shown in Figure 7.

The n and b data have been used to establish the time-temperature-transformation (T-T-T) diagram presented in Figure 8, for the 1025 steel. The diagram exhibits the start of the transformations, t_{AV_F} and t_{AV_P}, and the time for 99 pct transformation of the individual phases. It should be emphasized that the start time for the $\gamma' \rightarrow$ pearlite transformation is the same as the experimental time for completion of the $\gamma \rightarrow \alpha + \gamma'$ reaction. In addition, the $t_{0.99}$ pearlite line represents the time of 99 pct completion of the $\gamma' \rightarrow$ pearlite transformation.

It should also be noted that the helium gas cooling, which provided a cooling rate of 150 °C per second, limits the lowest attainable, truly isothermal data, to approximately 680 °C when the austenitizing temperature is 880 °C; at lower temperatures the relatively slow helium cooling allows the ferrite transformation to initiate prior to the attainment of the isothermal reaction temperature. The enhanced cooling rate derived from the pulsed water spray, 300 °C per second, permitted isothermal transformation kinetics to be obtained down to approximately 645 °C, this being the minimum temperature shown in Figure 8.

B. *Continuous-Cooling Measurements*

1. *CCT diagrams*

The time-temperature response for the 1025 steel measured at different continuous-cooling rates is shown in Figure 9. During initial cooling, prior to any transformation, the cooling was described by the following equation:

$$\ln\left(\frac{T - T_g}{T_{A_3} - T_g}\right) = -\frac{hA}{\rho VC_P}t \qquad [8]$$

which holds for a sample having negligible internal temperature gradients. From the measured transient temperature of the sample, the term $hA/\rho VC_P$ was found to be a function of temperature:

$$\frac{hA}{\rho VC} = a_0 + a_1(T - T_{A_3}) \qquad [9]$$

The start of the $\gamma \rightarrow \alpha + \gamma'$ transformation was taken to be the time at which the experimental cooling curve first deviates from that predicted by Eqs. [8] and [9] because upon initiation of the transformation the cooling rate decreases as the heat of transformation is evolved. The onset of the $\gamma \rightarrow \alpha + \gamma'$ transformation was also established from the diametral contraction of the austenite phase and the measured austenite thermal expansion coefficient.[1] A deviation from the predicted austenite behavior based simply on thermal contraction was taken to reflect the volume change associated with the onset of the ferrite reaction. The calculated "start time" for the $\gamma \rightarrow \alpha + \gamma'$ transformation, $t_{AV_{CCT\,F}}$, is shown in Figure 9. The "start time" for the same transformation under isothermal conditions is included in the diagram and is seen to be consistently less than the corresponding continuous-cooling transformation start time.

2. *Determination of continuous-cooling transformation kinetics for CCT data*

The fraction of each phase formed as a function of time was calculated from the measured diametral expansion data

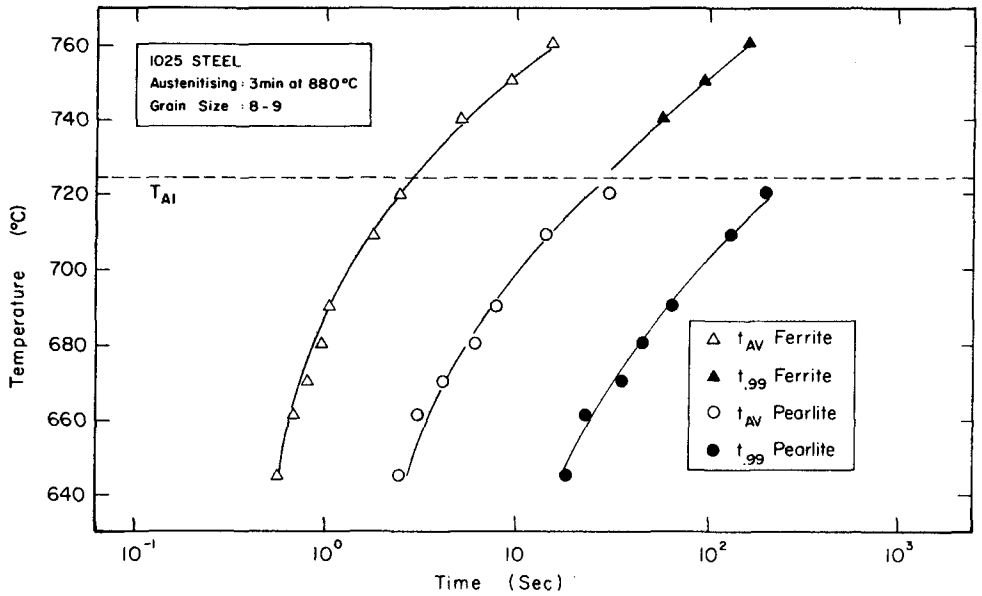

Fig. 8—Time-temperature-transformation (TTT) diagram for 1025 steel.

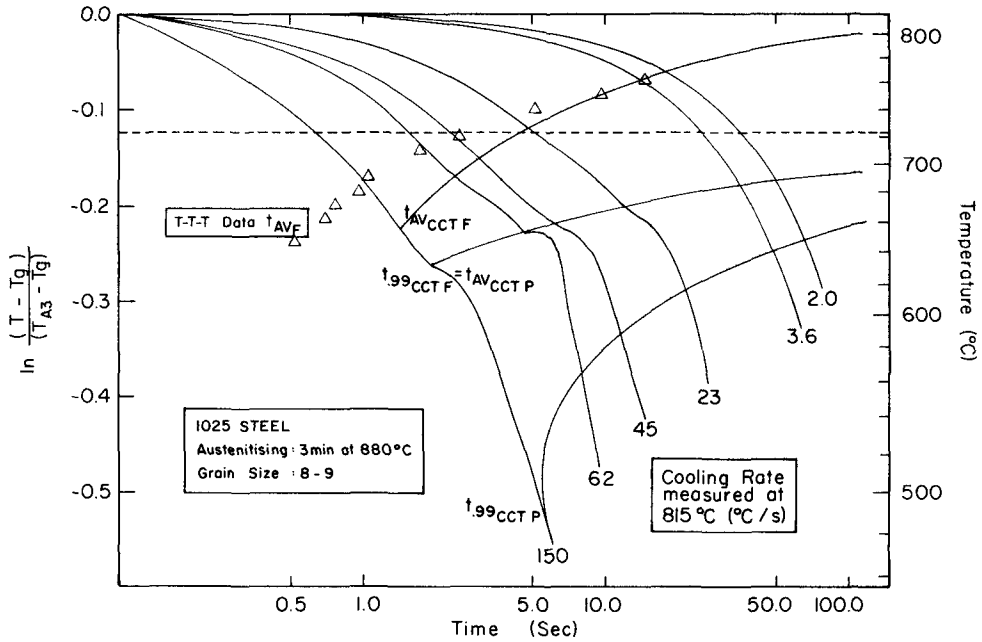

Fig. 9—Continuous-cooling transformation (CCT) diagram for 1025 steel.

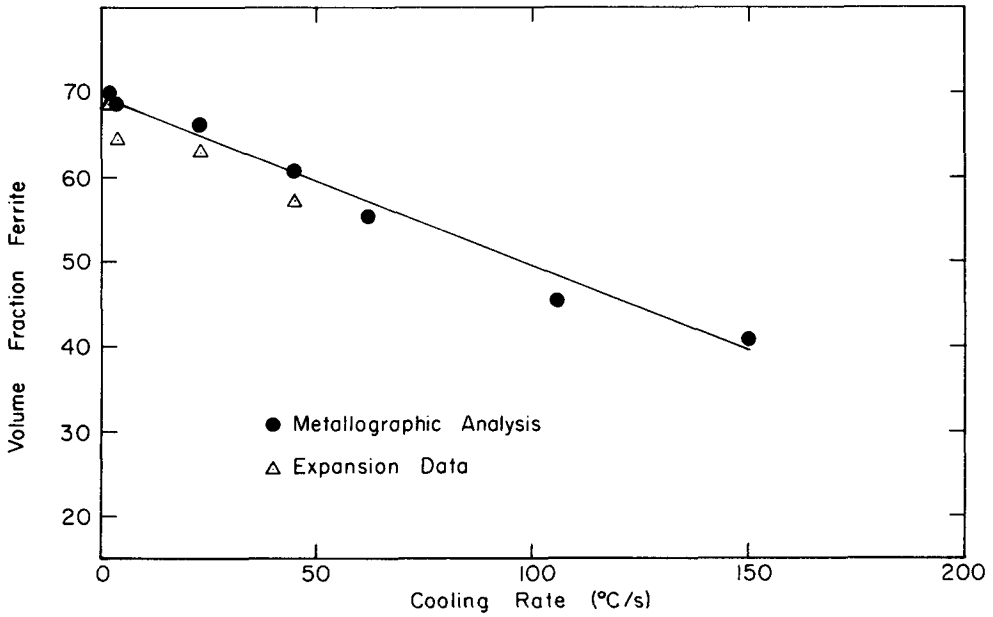

Fig. 10—Comparison of fraction of total ferrite formed as determined by expansion-coefficient analysis and by quantitative metallography.

and the thermal history of each CCT curve. This involved first correcting ΔD by subtracting the thermal contribution due to the continuous cooling. The expansion coefficient, α_{mix}, representing the transforming structure, was defined in terms of the fraction of austenite transformed, X_A. In the $\gamma \rightarrow \alpha + \gamma'$ transformation:

$$\alpha_{\text{mix}} = X_A\alpha_F(T) + (1 - X_A)\alpha_A(T) \qquad [10]$$

In the $\gamma' \rightarrow$ pearlite transformation:

$$\alpha_{\text{mix}} = X_{F_{\text{CCT}}}\alpha_F(T) + (X_A - X_{F_{\text{CCT}}})\alpha_P(T) + (1 - X_A)\alpha_A(T) \qquad [11]$$

where α_A, α_F, α_P are the expansion coefficients of the austenite, ferrite, and pearlite phases.[1]

The fraction of austenite transformed and the percentage of ferrite and pearlite present were obtained by first approximating the extent of the transformation, then making incremental changes until a fit was obtained with the thermal history curve. The total fraction of ferrite formed as a function of cooling rate was obtained from this analysis. This value was in good agreement with that obtained by quantitative metallographic examination of the structure following the continuous-cooling test. The results are shown in Figure 10.

The time for 99 pct completion of the transformations was determined by plotting the slope of the thermal and dilatometric continuous-cooling data, dT/dt, $d\Delta D/dt$ *vs* time. The transition between the completion of the ferrite transformation and the initiation of the pearlite reaction is seen as a point of slope change for both parameters. The 99 pct completion of the pearlite transformation, $t_{99_{\text{CCT}\,P}}$, is taken as that point where the dT/dt curve meets the constant dT/dt associated with the overall cooling rate, *i.e.*, the cooling rate as determined by Eqs. [8] and [9], unaffected by the heat of transformation. The values of $t_{99_{\text{CCT}\,F}}$ and $t_{99_{\text{CCT}\,P}}$ obtained in this manner are shown in Figure 9.

3. *The additivity rule*

The isothermal-transformation kinetics can be used to predict continuous-cooling transformations only if the instantaneous transformation rate is solely a function of the fraction transformed, X, and the transformation temperature, T. If this condition holds the transformation is additive, wherein the total time to reach a given stage of transformation is obtained by adding the fractions of the time required to reach this stage in isothermal increments until the sum equals unity.

$$\int_0^t \frac{dt}{t_A(T)} = 1$$

where t_A is the time required to reach X_A isothermally. In the previous study of the decomposition of austenite to pearlite in a eutectoid, plain-carbon steel it was found that this condition was satisfied if n was a constant for the transformation reaction and if b was solely a function of temperature.

To check if additivity holds for the hypoeutectoid steel, the following integrations were performed for the continuous-cooling conditions:

$$\int_{t_{\text{AV}_{\text{CCT}\,F}}}^{t_{99_{\text{CCT}\,F}}} \frac{dt}{t_{99_F}(T) - t_{\text{AV}_F}(T)} X_{F_E}(T) \qquad [12]$$

$$\int_{t_{\text{AV}_{\text{CCT}\,P}}}^{t_{99_{\text{CCT}\,P}}} \frac{dt}{[t_{99_P}(T) - t_{\text{AV}_P}(T)]}[1 - X_{F_E}(T)] \qquad [13]$$

$$\int_0^{t_{\text{AV}_{\text{CCT}\,F}}} \frac{dt}{t_{\text{AV}}(T)} \qquad [14]$$

Equations [12] to [14] correspond to the ferrite transformation, the pearlite transformation, and the incubation period preceding the transformation, respectively. The combined ferrite/pearlite and incubation plus ferrite transformations were also examined. The variables employed in the calculation and the integrations performed are shown in Figure 11. The results are contained in Table III and are compared with dilatometer results. Good agreement is obtained within the $\gamma \rightarrow \alpha + \gamma'$ and the $\gamma' \rightarrow$ pearlite transformation regions. However, calculation of the "start time" for the continuous-cooling transformation by integration

(a) $\gamma \rightarrow \alpha$ Transformation

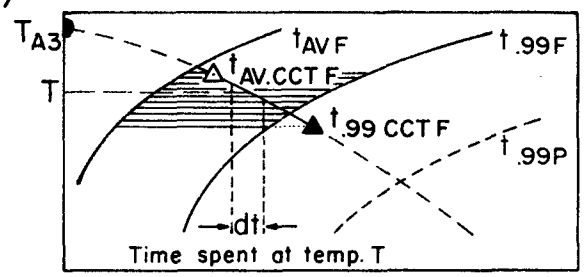

$$\int_{t_{AV\,CCT\,F}}^{t_{.99\,CCT\,F}} \frac{dt}{t_{.99F}(T) - t_{AVF}(T)} \times X_{F_E}(T) =$$

(b) $\gamma^{I} \rightarrow$ Pearlite Transformation

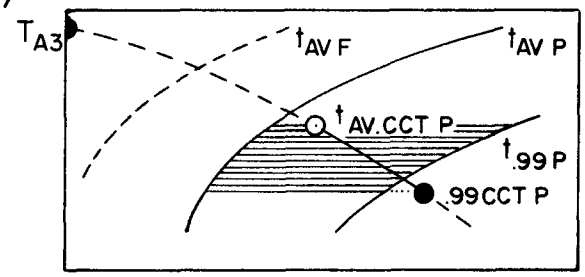

$$\int_{t_{AV\,CCT\,P}}^{t_{.99\,CCT\,P}} \frac{dt}{t_{.99P}(T) - t_{AVP}(T)} \times \left[1 - X_{F_E}(T)\right] =$$

(c) $\gamma \rightarrow \alpha$ Transformation + $\gamma^{I} \rightarrow$ Pearlite Transformation

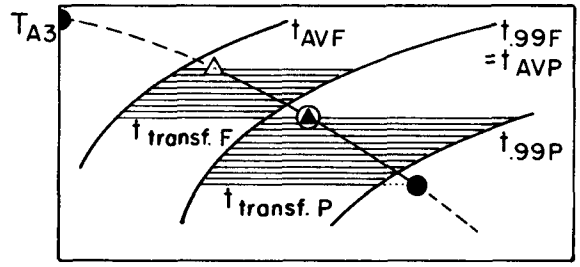

$$\int_{t_{AV\,CCT\,F}}^{t_{.99\,CCT\,F}} \frac{dt}{t_{.99F}(T) - t_{AVF}(T)} \times X_{F_E}(T) +$$

$$\int_{t_{AV\,CCT\,P}}^{t_{.99\,CCT\,P}} \frac{dt}{t_{.99P}(T) - t_{AVP}(T)} \times \left[1 - X_{F_E}(T)\right] =$$

(d) INCUBATION

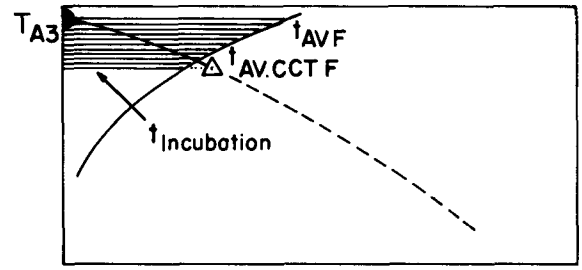

$$\int_{0}^{t_{AV\,CCT\,F}} \frac{dt}{t_{AV\,F}(T)} =$$

(e) INCUBATION + $\gamma \rightarrow \alpha$ Transformation

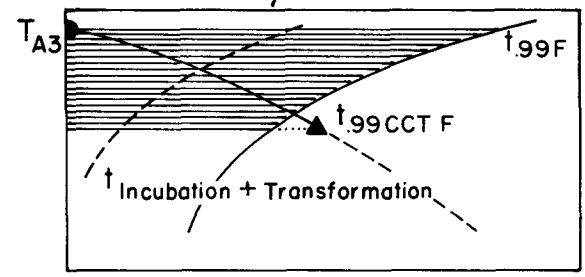

$$\int_{0}^{t_{.99\,CCT\,F}} \frac{dt}{t_{.99F}(T)} \times X_{F_E}(T) =$$

Fig. 11 — Diagrams showing the calculation of transformation and incubation times for continuous-cooling conditions.

Table III. Predictions of Incubation Time and Time to Transform 99 Pct Austenite Using Additivity Rule, Compared with Dilatometer Results

Prediction	Cooling Rate (°C/s)					
	2.0		3.6		23.0	
	Integ.	Dil.	Integ.	Dil.	Integ.	Dil.
(a) $\gamma \rightarrow \alpha$ transformation $\int_{t_{AVCCT\,F}}^{t_{99CCT\,F}} \frac{dt}{t_{99_F}(T) - t_{AV_F}(T)} X_{F_E}(T)$	0.654	0.686	0.645	0.660	0.630	0.648
(b) $\gamma' \rightarrow P$ transformation $\int_{t_{AVCCT\,P}}^{t_{99CCT\,P}} \frac{dt}{t_{99_P}(T) - t_{AV_P}(T)} [1 - X_{F_E}(T)]$	0.331	0.314	0.364	0.340	0.388	0.352
(c) $\gamma \rightarrow \alpha$ transformation + $\gamma' \rightarrow P$ transformation (a) + (b)	0.985	1.00	1.009	1.00	1.018	1.00
(d) Incubation* $\int_0^{t_{AVCCT\,F}} \frac{dt}{t_{AV_F}(T)}$	0.177	—	0.164	—	0.181	—
(e) Incubation + $\gamma \rightarrow \alpha$ transformation $\int_0^{t_{99CCT\,F}} \frac{dt}{t_{99_F}(T)} X_{F_E}(T)$	0.603	—	0.612	—	0.610	—

*This should equal 1 if the Scheil equation[7] is valid for the incubation period.

over the incubation period, as proposed by Scheil,[7] produces a serious overestimation. Reasonable agreement is observed for the combined incubation and ferrite transformation, but this simply reflects the dominance of the ferrite component of the integration in the calculation.

C. *Microstructural Assessment of the Nucleation Conditions*

In the eutectoid austenite-to-pearlite transformation the kinetic parameter, n, was found to be approximately 2 over the transformation temperature range 590 to 690 °C.[1] This was interpreted as reflecting rapid site saturation with predominant nucleation at three grain intersections (grain edges) after saturation of four grain intersections (grain corners). A metallographic analysis confirmed that the pearlite nucleated preferentially at grain boundaries (usually indistinguishable from grain corners and grain edges on a two-dimensional surface).

Metallographic examination also has been conducted on samples of the 1025 steel isothermally transformed to complete the austenite-to-ferrite transition but water-quenched* after a small amount of pearlite (5 to 10 pct) had formed. The ferrite was seen to nucleate preferentially on the preexisting austenite grain boundaries, as shown in Figure 12. The experimentally measured $n_F = 1.3$ would correspond to a theoretical nucleation condition of early site saturation with all particles growing from very small dimensions.[15] The early site saturation assures that there is only one dominant transformation process, temperature-dependent diffusion-controlled growth. Therefore, the additivity condition—that the fraction transformed is dependent only on the fraction already present and the transformation temperature—may be satisfied, although the degree of soft impingement (overlap of the carbon diffusion fields) would also be expected to affect the kinetics at any temperature.

*The controlled-temperature dilatometer equipment permits the rapid quenching of the steel at any stage of the transformation by flushing a stream of water through the cylindrical sample.

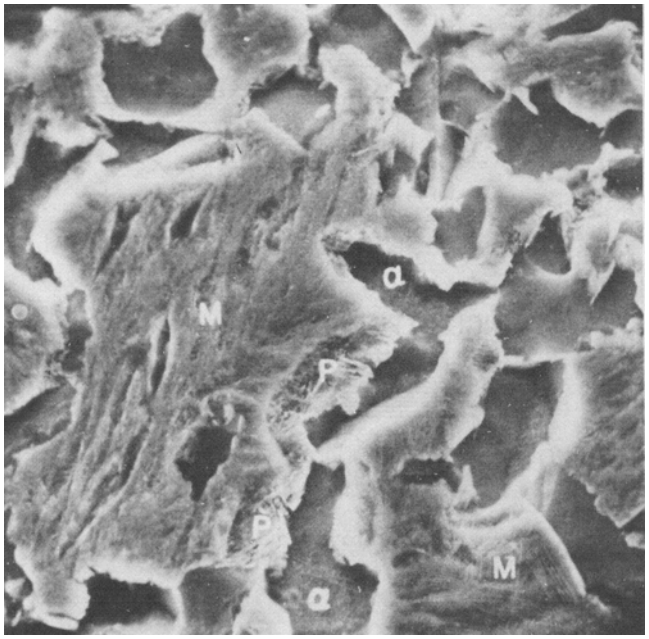

Fig. 12—1025 steel partially transformed at 655 °C showing ferrite at the austenite grain boundaries, pearlite growing on the ferrite, and a matrix of quenched austenite transformed to martensite. Nital etch. Magnification 3720 times (Scanning Electron Microscope).

The morphology of the grain boundary ferrite was observed to change from an equiaxed product characteristic of growth at high temperatures ($T_{A_1} < T_{A_3}$) to an elongated Widmanstätten precipitate at $T < T_{A_1}$.

The experimentally measured value of the pearlite kinetics parameter, $n_p \simeq 1$, also implies a condition of early site

saturation. This is consistent with observed preferential nucleation at the grain boundary ferrite-austenite interface.

D. *Application of Isothermal Data to Predict Continuous-Cooling Transformation*

The approach taken by Agarwal and Brimacombe[2] was previously adopted to describe the continuous-cooling kinetics of the eutectoid carbon steel and has been applied to the hypoeutectoid steels. Continuous-cooling rates of 2.0, 3.6, and 23 °C per second have been examined.

The procedure involves dividing the continuous-cooling curve into small time segments (0.25 second for 23 °C per second and 1 second for 2.0 and 3.0 °C per second). The fraction of austenite transformed then is calculated assuming additive isothermal conditions for each time segment. The calculation of fraction of ferrite formed is initiated at $t_{AV_{CCT\,F}}$, and uses the n_F and ln $b_F(T)$ determined from the TTT data as shown in Figure 13. In the first time segment, at temperature T_1, the fraction of ferrite formed (normalized to X_{F_1}) is calculated as follows:

$$X_{F_1} = 1 - \exp[-b_F(T)t_1^{n_F}] \quad [15]$$

where t_1 = the first time increment, Δt, after $t_{AV_{CCT\,F}}$. This value is then corrected to the fraction of austenite transformed by:

$$X_{A_1} = X_{F_C}(T_1)X_{F_1} \quad [16]$$

In the second cooling segment, since each isothermal temperature would produce a different fraction of ferrite, it is first necessary to change X_{F_1} to its equivalent fraction at T_2.

$$X'_{F_1} = \frac{X_{F_C}(T_1)}{X_{F_C}(T_2)}X_{F_1} \quad [17]$$

Then the time required to produce X'_{F_1} at T_2 is calculated, t'_2, using n_F and ln $b_F(T_2)$

$$t'_2 = \left[\frac{\ln \dfrac{1}{1 - X'_{F_1}}}{b_F}\right]^{1/n_F} \quad [18]$$

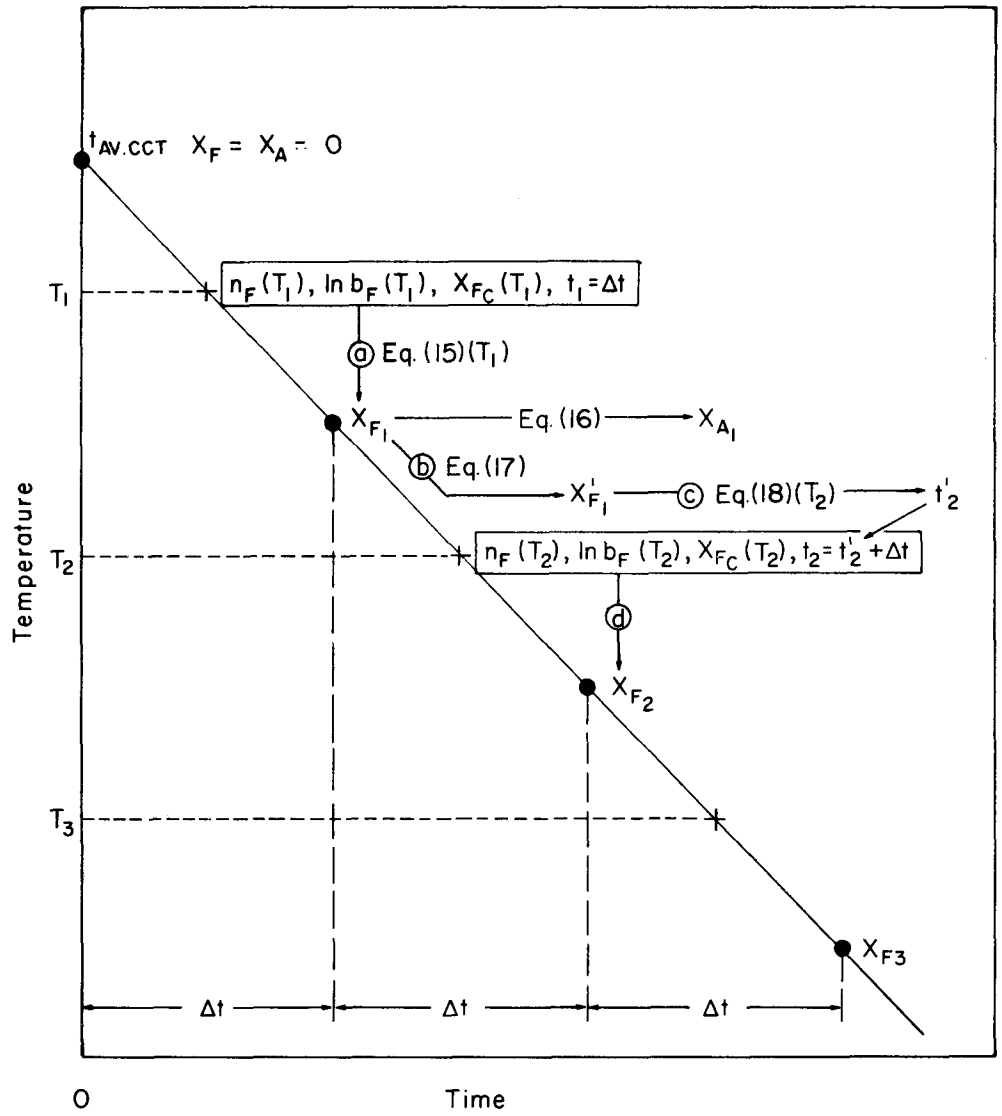

Fig. 13—Diagram showing the calculation for applying isothermal transformation data to predict continuous-cooling transformation kinetics.

The time segment, Δt, is added to this calculated value and a new fraction of ferrite, X_{F_2}, is calculated. X_{F_2} is converted to the fraction of austenite transformed using the T_2 equivalent of Eq. [16]. This procedure is repeated until the ferrite transformation is finished, as determined by $t = t_{AV_{CCT\,P}}$.

The same procedure is followed to predict the pearlite transformation kinetics. In the first time segment, t_1, after $t_{F_{CCT\,F}}$ (or $t_{AV_{CCT\,P}}$) at temperature T_P, the fraction pearlite is calculated using n_P and ln $b_P(T_{P_1})$

$$X_{P_1} = 1 - \exp[-b_P(T_{P_1})t_1^{n_P}] \quad [19]$$

This value then is corrected to the incremental fraction of austenite transformed

$$X'_A = [1 - X_{F_E}(T_P)]X_{P_1} \quad [20]$$

where the total fraction of austenite transformed is

$$X_A = X'_A + X_{A_F} \quad [21]$$

and X_{A_F} ($=X_{F_E}$) is the total fraction of austenite decomposed in the $\gamma \rightarrow \alpha + \gamma'$ transformation. In the second time segment for the pearlite transformation at T_{P_2}, the X_{P_1} must be corrected to a value appropriate for T_{P_2}

$$X'_{P_1} = \frac{1 - X_{F_E}(T_{P_1})}{1 - X_{F_E}(T_{P_2})} X_{P_1} \quad [22]$$

The time required to produce X'_{P_1} of pearlite at T_{P_2} is calculated using n_P and ln b_P (T_{P_2}) and is added to the time segment at T_{P_2}. A new fraction of pearlite X_{P_2} is calculated using n_P and ln b_P (T_{P_2}). This procedure is repeated until all the austenite is transformed, *i.e.*, $X_A = 1.0$.

The resulting calculated X_A *vs* time, the predicted transformation kinetics of the austenite decomposition, was compared with its experimental counterpart obtained by analysis of the diametral expansion, using the expansion-coefficient of each of the component phases. The results for the 2.0, 3.6, and 23 °C per second cooling rates are shown in Figures 14, 15, and 16, respectively. The results in all three cases exhibit excellent agreement.

Additional tests are being performed to examine the effect of discontinuous changes in cooling rate during the continuous-cooling of the steel. Continuous processing of a steel rod on a Stelmor line could involve partial transformation in the intercritical region between T_{A_3} and T_{A_1}, rapid cooling and subsequent completion of the transformation at temperatures below T_{A_1}. Since the composition of the austenite that results during precipitation of ferrite is dependent on the reaction temperature and the resulting extent of the carbon gradient (degree of soft impingement) also is affected by the temperature, the final decomposition kinetics may be a function of the initial transformation temperature. The transformation would not be additive in this situation. However, the excellent agreement between the predicted and the measured transformation kinetics as seen in Figures 14 to 16 shows that this is not a problem for normal continuous-cooling conditions.

IV. SUMMARY

The decomposition kinetics of austenite-to-ferrite plus pearlite in a hypoeutectoid, 1025 steel have been determined by diametral dilatometric measurements on a thin-walled cylindrical specimen. Cooling rates of 150 °C per second, obtained by combining internal and external flow of helium gas, and 300 °C per second by combining an internal pulsed water spray with an external flow of helium gas, limited achievable minimum isothermal transformation temperatures to approximately 680 and 645 °C, respectively. Isothermal transformation kinetics were characterized in terms of the Avrami equation to yield the n and b parameters and a transformation-start time. n was found to be independent of temperature, indicating a constant nucleation condition.

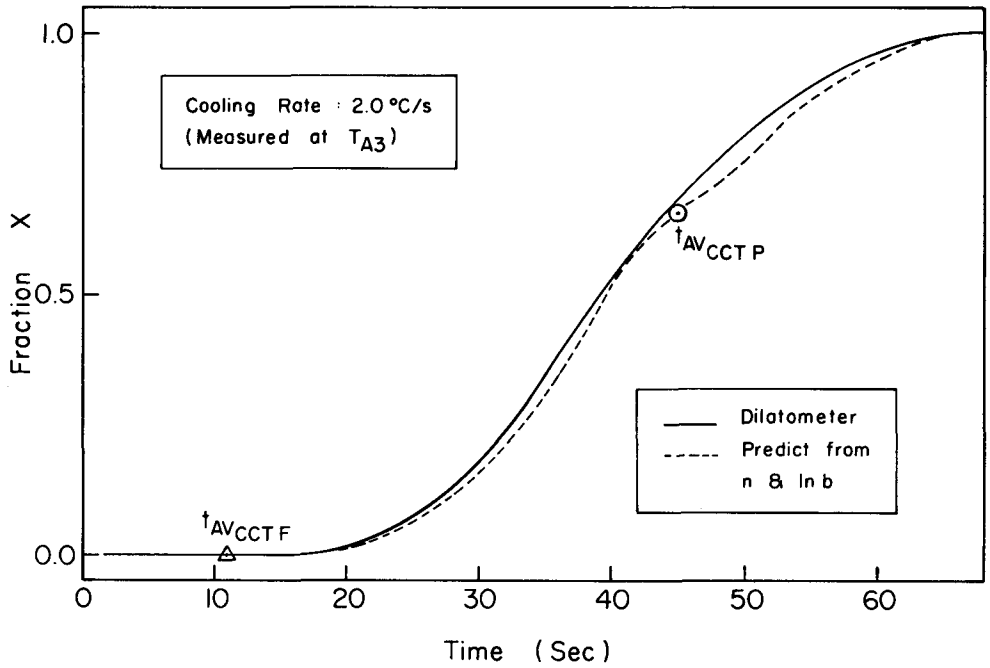

Fig. 14—Predicted X_A *vs* time compared with equivalent results obtained from the expansion analysis of the dilatometric curve for the 2.0 °C/s cooling rate.

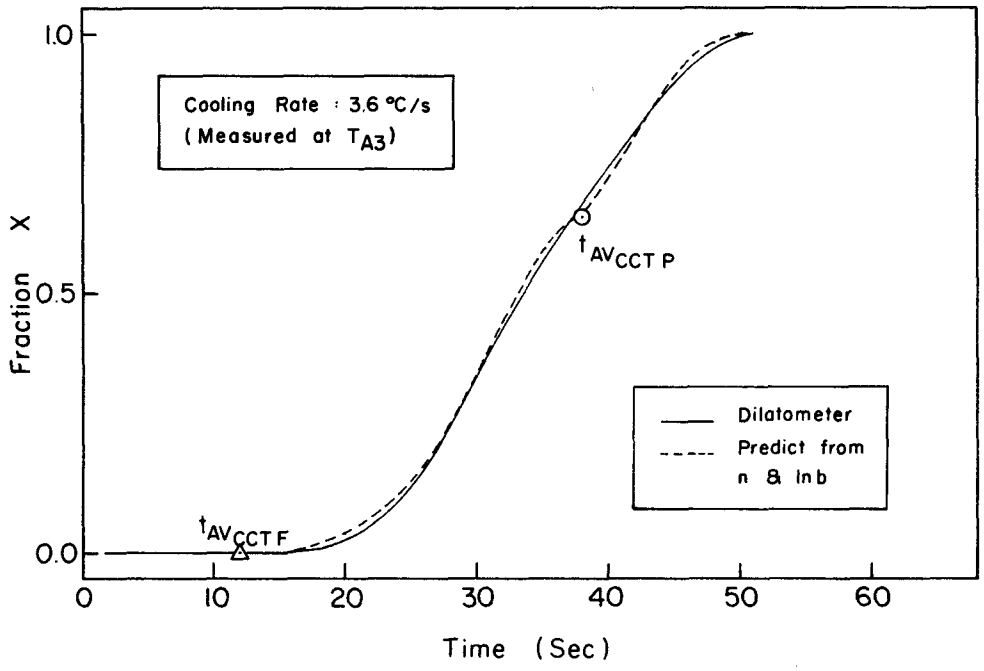

Fig. 15—Predicted X_A *vs* time compared with equivalent results obtained from the expansion analysis of the dilatometric curve for the 3.6 °C/s cooling rate.

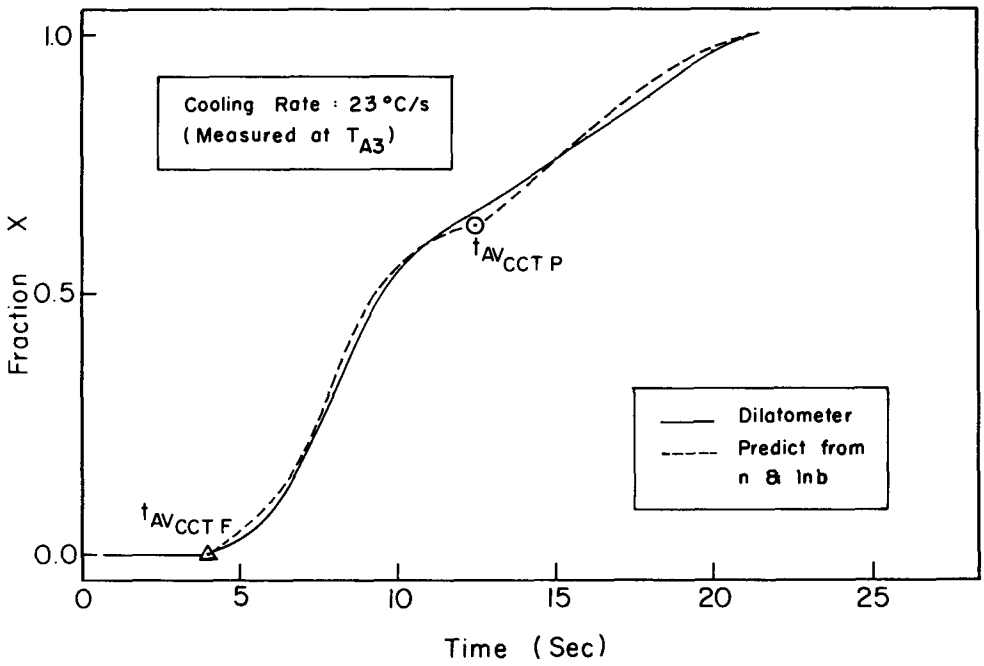

Fig. 16—Predicted X_A *vs* time compared with equivalent results obtained from the expansion analysis of the dilatometric curve for the 23.0 °C/s cooling rate.

The Additivity Principle has been checked and applies well to the transformation period of the ferrite and pearlite reactions but it does not hold for the incubation period.

The isothermal kinetics data and the CCT transformation-start time have been fed to a mathematical model to predict, using the Additivity Principle, the continuous-cooling transformation of the steel. Excellent agreement was obtained with the measured continuous-cooling kinetics for cooling rates of 2 to 23 °C per second.

NOMENCLATURE

A	Surface area transferring heat, m^2
α	Ferrite
α_A	Expansion coefficient of austenite, mm/mm °C
α_F	Expansion coefficient of ferrite, mm/mm °C
α_{mix}	Mixed expansion coefficient based on the volume fraction of each phase present, mm/mm °C
α_P	Expansion coefficient of pearlite, mm/mm °C

b Kinetic parameter from Avrami equation
b_F Kinetic parameter for ferrite transformation
b_P Kinetic parameter for pearlite transformation
C_P Specific heat of sample, kJ/kg °C
C_α Wt pct C in α
C_γ Wt pct C in γ
C_c Wt pct carbon
ΔD_F Diameter change due to transformation of austenite to ferrite, mm
ΔD_P Diameter change due to transformation of austenite to pearlite, mm
ΔD_T Total diameter change due to complete transformation, mm
γ Austenite having a 0.25 pct carbon content
γ' Austenite having an increased carbon content due to ferrite precipitation
h Surface heat transfer coefficient, kW/m^2 °C
n Kinetic parameter from Avrami equation
n_F Kinetic parameter for ferrite transformation
n_p Kinetic parameter for pearlite transformation
P Pearlite
ρ Density, kg/m^3
T Temperature, °C
T_g Temperature of cooling gas, °C
t Time, s
t_{AV} t_{AVRAMI}, the transformation start time as determined by a best least-squares fit
t_{AV_F} Start of isothermal $\gamma \rightarrow \alpha + \gamma'$ transformation
t_{AV_P} Start of isothermal $\gamma' \rightarrow$ pearlite transformation
$t_{AV_{CCT\,F}}$ Start time for $\gamma \rightarrow \alpha + \gamma'$ transformation under continuous-cooling conditions
$t_{AV_{CCT\,P}}$ Start time for $\gamma' \rightarrow$ pearlite transformation under continuous-cooling conditions
t_x Isothermal time to a given fraction transformed, s
t_1 Time at 1st isothermal increment describing continuous-cooling curve, s
t_2' Time to produce volume fraction X_{F_1}, at T_2, s
t_{99_F} Isothermal time to reach 0.99 volume fraction of ferrite, s
t_{99_P} Isothermal time to reach 0.99 volume fraction of pearlite, s
dt Increment of time during continuous cooling, s
τ Isothermal time to start of transformation, s
V Volume, m^3
W_F Weight fraction of ferrite
X Volume fraction transformed
X_A Volume fraction of austenite transformed
X_F Volume fraction of ferrite normalized to a base of 1.0
X_F^o Total volume fraction of ferrite obtained from metallographic analysis
X_{F_c} Calculated total volume fraction of ferrite based on a phase boundary extrapolation
X_{F_E} Total volume fraction of ferrite based on experimental dilatometer data
$X_{F\,CCT}$ Volume fraction of ferrite based on continuous-cooling experiments
X_{F_1} Volume fraction of ferrite formed at T_1
X'_{F_1} Volume fraction of ferrite formed at T_1 but cooled and now present at T_2
X_{F_2} Volume fraction of ferrite formed at T_2
X_P Volume fraction of pearlite normalized to a base of 1.0

ACKNOWLEDGMENT

The authors are indebted to the American Iron and Steel Institute who have provided full financial support (Grant No. 62-446) for this study.

REFERENCES

1. E. B. Hawbolt, B. Chau, and J. K. Brimacombe: *Metall. Trans. A*, 1983, vol. 14A, pp. 1803-15.
2. M. Avrami: *J. Chem. Phys.*, 1940, vol. 8, pp. 212-24.
3. P. K. Agarwal and J. K. Brimacombe: *Metall. Trans. B*, 1981, vol. 12B, pp. 121-33.
4. J. Iyer: M.A.Sc. Thesis, The University of British Columbia, Vancouver, BC, Canada, 1983.
5. M. Umemoto, N. Nishioka, and I. Tamura: *J. Heat Treating*, 1981, vol. 2, no. 2, pp. 130-38.
6. M. Umemoto, K. Horiuchi, and I. Tamura: *Trans. ISIJ*, 1982, vol. 22, pp. 854-61.
7. E. Scheil: *Archiv. für Eissenhuttenwesen*, 1935, vol. 12, pp. 565-67.
8. J. S. Kirkaldy: *Metall. Trans.*, 1973, vol. 4, pp. 2327-33.
9. J. S. Kirkaldy and R. C. Sharma: *Scripta Metallurgica*, 1982, vol. 16, pp. 1193-98.
10. R. Blondeau, P. H. Maynier, J. Dollet, and B. Veillard-Baran: *Proceedings of the 16th International Heat Treating Conference, Heat Treatment '76*, 1976, pp. 189-200.
11. T. Gladman, I. D. McIvor, and F. B. Pickering: *J. Iron and Steel Inst.*, 1972, vol. 210, pp. 916-30.
12. W. Heller: *Rail Steels*, STP 644, ASTM, Philadelphia, PA, 1978, p. 162.
13. K. W. Andrews: *J. Iron and Steel Inst.*, 1965, vol. 203, pp. 721-27.
14. L. Kaufman, S. V. Radcliffe, and M. Cohen: in *Decomposition of Austenite by Diffusional Processes*, V. F. Zackay and H. I. Aaronson, eds., Interscience Publ., 1962, pp. 313-52.
15. J. W. Christian: *The Theory of Transformations in Metals and Alloys*, Pergamon Press, 1975, pp. 535-48.